Adaptation of OFDM under Visible Light Communications and Illumination Constraints*

T.D.C. Little and H. Elgala
Multimedia Communications Laboratory
Department of Electrical and Computer Engineering
Boston University, Boston, Massachusetts
{*tdcl,helgala*}@*bu.edu*

October 2, 2014

MCL Technical Report No. 10-02-2014

Abstract– Orthogonal frequency division multiplexing (OFDM) is increasingly studied and adopted as a modulation technique for RF and optical communication systems. In this paper, we investigate challenges to the adoption of OFDM for use in lighting systems that support both intensity control and data communication based on the visible light communication (VLC) technology. In particular, we survey the requirements for energy efficiency, intensity control (dimming) and light-emitting diode (LED) driver integration in lighting systems. These requirements are mapped to contemporary and novel OFDM adaptations to show how both the lighting and communications needs can be met in dual-use scenarios while preserving both missions with reasonable performance.

Keywords: Optical communication, VLC, LED, OFDM, nonlinearity, dimming.

*In *Proc. Asilomar Conf. on Signals, Systems, and Computers*, November 2-5, 2014, CA. This work is supported by the NSF under grant No. EEC-0812056. Any opinions, findings, and conclusions or recommendations expressed in this material are those of the author(s) and do not necessarily reflect the views of the National Science Foundation.

1 Introduction

Advances in solid-state lighting (SSL) are enabling LEDs to be the primary illumination source of the future [1]. The adoption of LEDs aims to significantly reduce energy consumption and facilitate precise intensity and color control of illuminated spaces [2]. Two methods are generally utilized to produce the white light in LED-based luminaries [3]. The least expensive and most popular is phosphor conversion, in which a blue LED is coated with phosphor to emit broad-spectrum white light. The second approach offers color-tunable lighting through combining monochromatic LEDs of different colors to produce white via color mixing. Besides the several advantages of LEDs, they also have fast response times making them excellent light sources for high-speed VLC links in which data is transmitted wirelessly from LED-based luminaries through invisible intensity variations [4]. In VLC systems, the communication signal is modulated onto the instantaneous power of the optical carrier and the optical detector generates a current proportional to the received instantaneous power, *i.e.*, direct intensity modulation with direct detection (IM/DD) [5].

VLC research to date has primarily been focused on achieving increasingly high data rates [6, 7]. The spectrally-efficient OFDM constitutes a hot research topic in the field of VLC [8]. In OFDM-based VLC systems, high data rates are supported through parallel transmission of complex constellations on orthogonal sub-carriers. Assuming near-field communication in a static scenario, recent experimental setups have been demonstrated to achieve Gbps VLC links using commercial off-the-shelf components [9]. According to the laboratory conditions of these demonstrations, the human factors component and illumination features for a realistic illumination and communication system have been largely overlooked. Paramount to the practical challenges of VLC is ensuring dimming functionality while maintaining a reliable broadband communication link. In the literature, to our knowledge, demonstrating the illumination compatibility with high-speed communication remains an open challenge.

Recent research efforts are conducted to assist in developing modulation techniques which address the challenge of incorporating broadband VLC with high-quality illumination and lighting state control. In [10], time-domain OFDM symbols are transmitted onto the pulse width modulation (PWM) signal only during the "on-state." Here the data throughput is limited to the relatively low PWM line rate. In [11], the LED drive current is the time-domain OFDM signal multiplied by a periodic PWM pulse train. Here the practical communication is only feasible when the PWM signal is at least twice the frequency assigned to the largest OFDM sub-carrier frequency, *i.e.* inter-carrier interference (ICI) for slower PWM rates. This constraint diminishes the feasibility of industry compatible dimmed broadband VLC link as PWM frequencies of off-the-shelf LED drivers are in KHz.

In contrast, our work proposes a novel approach to (1) utilize the entire PWM cycle for data transmission instead of limiting the transmission to be only during the "on-state," *i.e.*, the data throughput is not limited by the PWM frequency, (2) use the full LED dynamic range of operation to minimize the nonlinear distortion (mainly clipping) of the OFDM signal, *i.e.*, DC biasing is not required and the linear range of operation is extended, and (3) maintain a high link capacity for a wide dimming range, *i.e.* the signal-to-noise ratio (SNR) is independent on the dimming level within that wide range.

The remainder of this paper is organized as follows. PWM dimming and two OFDM versions that are suitable for IM/DD are highlighted in Section II. VLC system constraints are discussed in Section III. In Section IV, our proposed approach is introduced together with signal quality deter-

mination and perceived brightness calculation. The achieved system performance based on simulation results and experimental measurements is presented in Section V. Conclusions are drawn in Section VI.

2 Optical OFDM Generation and Dimming Functionality

The building blocks of a VLC compatible OFDM transmitter are shown in Fig. 1. The data is an input stream of grouped ones and zeros "bit-symbols" based on the considered quadrature amplitude modulation (QAM) or phase shift keying (PSK) constellations. The generated complex "QAM/PSK-symbols" are then mapped onto a vector X_k. After taking the IFFT of the vector X_k, a cyclic prefix (CP) is added to the real time-domain OFDM symbol to avoid multipath induced inter-symbol interference (ISI). In order to simplify the analysis, the CP is ignored and the current signal driving the LED can be written as:

$$i_{\text{OFDM}}(t) = x_n = \frac{1}{N}\sum_{k=1}^{N} X_k \exp^{\left(j\frac{2\pi}{N}nk\right)}, 0 \leq t \leq T \tag{1}$$

where, $x_n, n = 0, \cdots, N-1$ are the N time-domain output samples, the values $X_k, k = 0, \cdots, N-1$ are the N frequency-domain input symbols and T is the duration of an OFDM symbol.

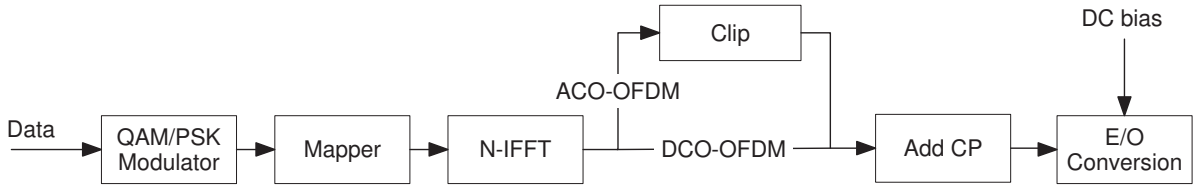

Figure 1: Building blocks DCO-OFDM and ACO-OFDM transmitters.

In case of the DC-biased optical OFDM (DCO-OFDM) [12],

$$X_k = \left[\ 0 X_1 X_2\ \cdots\ X_{N/2-1}\ 0\ X^*_{N/2+1}\ \cdots\ X^*_2 X^*_1\right]^T \tag{2}$$

where, $(.)^*$ denotes the complex conjugate and $(.)^T$ denotes the transpose of a vector. The QAM/PSK-symbols are mapped to both odd and even indexed subcarriers of the length N IFFT operation. The Hermitian symmetry property of the vector X_k is needed to insure real-valued output signal, *i.e.* $X_k = X^*_{N-k}$. The values of the X_0 and the $X_{N/2}$ subcarriers are set to zero to ensure the Hermitian property. However, such DCO-OFDM signal generated in the time-domain is still bipolar, *i.e.* DC bias is required for proper operation where the bipolar signal is superimposed on this DC operating point.

Significant efforts are devoted to designing optical OFDM formats which are purely unipolar. All well-known solutions that do not require interference estimation and cancelation at the receiver must scarify half the spectral efficiency, *i.e.* the data rates are halved compared to DCO-OFDM. These solutions include the asymmetrically clipped optical OFDM (ACO-OFDM) [12]. In case of the ACO-OFDM,

$$X_k = \left[\ 0 X_1 0 X_2\ \cdots\ X_{N/2-1}\ 0\ X^*_{N/2+1}\ \cdots\ X_2 0 X^*_1\right]^T \tag{3}$$

Since X_k contains data only on the odd indexed subcarriers, the generated time-domain signal has a half-wave symmetry. The half-wave symmetry means that the same information in the first $N/2$ samples is repeated in the second half of the OFDM symbol. As a consequence, the negative part can be clipped without any loss of information. This clipping produces a unipolar signal. The intermodulation caused by clipping occurs only in the even indexed subcarriers and does not affect the data-carrying odd indexed subcarriers.

Lighting controls can increase the value of commercial buildings by making them more productive, comfortable, and energy-efficient [13]. This is often a product of dimming functionality, which is space and application specific. Thus, brightness control is an essential illumination function that must be incorporated in VLC systems. The principle of brightness control is to set the average amplitude of the forward current through the LED. Let ϕ_{SB} denote the target emitted average optical power, which is determined by the dimming level set point, and let I_{SB} denote the corresponding average forward current. There are two conventional schemes to implement brightness control: (1) biasing adjustment and (2) PWM.

Analog dimming, also known as amplitude modulation (AM) or continuous current reduction, is the simplest type of dimming control. This technique lessens the current amplitude linearly to adjust the radiated optical flux. Unfortunately, AM is prone to inducing a noticeable change in color ("color shift") [14]. For large number of subcarriers, the OFDM signal can be accurately modeled by a Gaussian random process with a zero mean value and a variance σ^2_{OFDM}. The average value of the biased DCO-OFDM signal $x[n]$ is equal to the bias current I_{DC}, *i.e.* average DCO-OFDM current $I_{\text{DCO-OFDM}}$ is zero. In the biasing adjustment method, it is straightforward to set the biasing level equal to I_{DC} for each DCO-OFDM symbol. In case of ACO-OFDM, $I_{\text{SB}} = I_{\text{DC}} + I_{\text{ACO-OFDM}}$, where $I_{\text{ACO-OFDM}}$ is the average ACO-OFDM current.

In digital dimming, the average duty cycle or signal density represents the equivalent analog dimming level, *i.e.* a digitally modulated pulse train yields the same average LED forward current as achieved using the analog technique. PWM is the simplest example of digital dimming modulation. The time period of the PWM signal is fixed, whereas the duty cycle D varies proportionally to the required dimming percentage. The classic case switches between an 'on' (high) and an 'off' (low) state. PWM is preferred in the industry due to its simplicity and inherent linearly as compared to AM and its reduced susceptibility to chromaticity shift [14].

A PWM signal current $i_{\text{PWM}}(t)$ with pulse width T and period T_{PWM} can be expressed as,

$$i_{\text{PWM}}(t) = \begin{cases} I_{\text{H}}, & 0 \leq t < T \\ I_{\text{L}}, & T < t \leq T_{\text{PWM}} \end{cases} \tag{4}$$

where I_{H} is the high level "on-state" which is assumed to be the maximum allowed LED drive current, I_{L} is the low level "off-state" which is assumed to be the minimum LED drive current (threshold or turn-on current) and $D = T/T_{\text{PWM}}$. Combinations of both AM and PWM in hybrid techniques have been proposed for even further reduction of perceived chromaticity shifts.

3 VLC System Constraints

3.1 LED Dynamic-Range

The dynamic-range (DR) of LEDs, DR_{LED}, is a main constraint for OFDM-based VLC. Each LED has a minimum recommended forward current according to the data sheet, which is the onset

of current flow and light emission. Due to thermal aspects, AC/pulsed currents must be limited according to the manufacturer's data sheet to ensure that the LED chip does not overheat, in order to avoid optical-to-electrical efficiency degradation or, in the worst case, total failure. Assuming a predistorter to linearize the LEDs' input-output characteristic, the LED outputs light that is linear with the drive current, where the limit is determined by I_{L} and I_{H} [5]. Thus, the LED behavior relating $i_{\mathrm{LED}}(t)$ to the output optical power $\phi_{\mathrm{LED}}(t)$ can be described as follows:

$$i_{\mathrm{LED}}(t) = \begin{cases} I_{\mathrm{H}} & \text{if } i_{\mathrm{LED}}(t) \geq I_{\mathrm{H}} \\ i_{\mathrm{LED}}(t) & \text{if } I_L < i_{\mathrm{LED}}(t) < I_{\mathrm{H}} \\ I_{\mathrm{L}} & \text{if } i_{\mathrm{LED}}(t) \leq I_{\mathrm{L}} \end{cases} \tag{5}$$

Therefore, the system is limited by $\mathrm{DR}_{\mathrm{LED}}$, which is denoted as,

$$\mathrm{DR}_{\mathrm{LED}} = I_{\mathrm{H}} - I_{\mathrm{L}} \tag{6}$$

By defining the DR of $i_{\mathrm{LED}}(t)$ as,

$$\mathrm{DR}_{\mathrm{OFDM}} = \max\{x[n]\} - \min\{x[n]\} \tag{7}$$

$\mathrm{DR}_{\mathrm{OFDM}}$ should be constrained by $\mathrm{DR}_{\mathrm{LED}}$, *i.e.* $\mathrm{DR}_{\mathrm{OFDM}} \leq \mathrm{DR}_{\mathrm{LED}}$.

3.2 Average Emitted Power and Peak-to-Average Power Ratio

Since the optical intensity cannot be negative, $i_{\mathrm{LED}}(t)$ must be nonnegative, *i.e.* $i_{\mathrm{LED}}(t) > 0$. The contribution of $i_{\mathrm{OFDM}}(t)$ to $\phi_{\mathrm{LED}}(t)$ is defined as,

$$\phi_{\mathrm{OFDM}}(t) = E[i_{\mathrm{OFDM}}(t)] \tag{8}$$

where $E[.]$ denotes statistical expectation. Due to the limit on power consumption, eye safety regulation and dimming requirement, the system usually operates under some average optical power constraint ϕ_{SB}, *i.e.* $\phi_{\mathrm{LED}}(t) \leq \phi_{\mathrm{SB}}$.

The contribution of $i_{\mathrm{OFDM}}(t)$ to $\phi_{\mathrm{LED}}(t)$ is set based on a linear scaling such that

$$i_{\mathrm{OFDM}}(t) = m \cdot i_{\mathrm{OFDM}}(t) \tag{9}$$

where, m is real-valued. The resulting signal has a standard deviation,

$$\sigma_{\mathrm{OFDM}} = m \cdot \sqrt{E[i^2_{\mathrm{OFDM}}(t)]} \tag{10}$$

σ_{OFDM} can be maximized by selecting a scaling factor with the greatest absolute value. To ensure that $i_{\mathrm{LED}}(t)$ stays within $\mathrm{DR}_{\mathrm{LED}}$, the greatest value of m is,

$$m = \frac{\mathrm{DR}_{\mathrm{LED}}}{\max\{i_{\mathrm{OFDM}}(t)\}} = \frac{I_H - I_L}{\max\{i_{\mathrm{OFDM}}(t)\}} \tag{11}$$

We define the illumination-to-communication efficiency (ICE) to quantify the contribution of the OFDM signal to I_{SB},

$$\mathrm{ICE} = \frac{\sigma_{\mathrm{OFDM}}}{I_{\mathrm{SB}}} \tag{12}$$

The dimming efficiency (DE) is also defined to relate the I_{SB} to the available DR_{LED},

$$\text{DE} = \frac{I_{\text{SB}}}{I_{\text{H}} - I_{\text{L}}} = \frac{I_{\text{SB}}}{\text{DR}_{\text{LED}}} \tag{13}$$

The real-valued time-domain OFDM signal envelope is still characterized by a high peak-to-average power ratio (PAPR) and remains a design challenge. The PAPR is defined as

$$\text{PAPR} = \frac{\max\{x^2[n]\}}{E[x^2[n]]} \tag{14}$$

Using Equ. (11), Equ. (13) and Equ. (14) in Equ. (12),

$$\begin{aligned} \text{ICE} &= \frac{m \cdot \sqrt{E[i^2_{\text{OFDM}}(t)]}}{I_{\text{SB}}} \\ &= \frac{\sqrt{E[i^2_{\text{OFDM}}(t)]}}{I_{\text{SB}}} \frac{I_H - I_L}{\max\{i_{\text{OFDM}}(t)\}} = \frac{1}{\text{DE} \cdot \sqrt{\text{PAPR}}} \end{aligned} \tag{15}$$

It is observed that ICE depends on three parameters: (1) brightness level, (2) LED dynamic range and (3) PAPR.

4 The Optical RPO-OFDM

In this work, it is proposed to combine $i_{\text{OFDM}}(t)$ with $i_{\text{PWM}}(t)$ as follows:

$$i_{LED}(t) = \begin{cases} i_{\text{PWM}}(t) - m \cdot i_{\text{OFDM}}(t), & 0 \le t \le T \\ i_{\text{PWM}}(t) + m \cdot i_{\text{OFDM}}(t), & T < t \le T_{\text{PWM}} \end{cases} \tag{16}$$

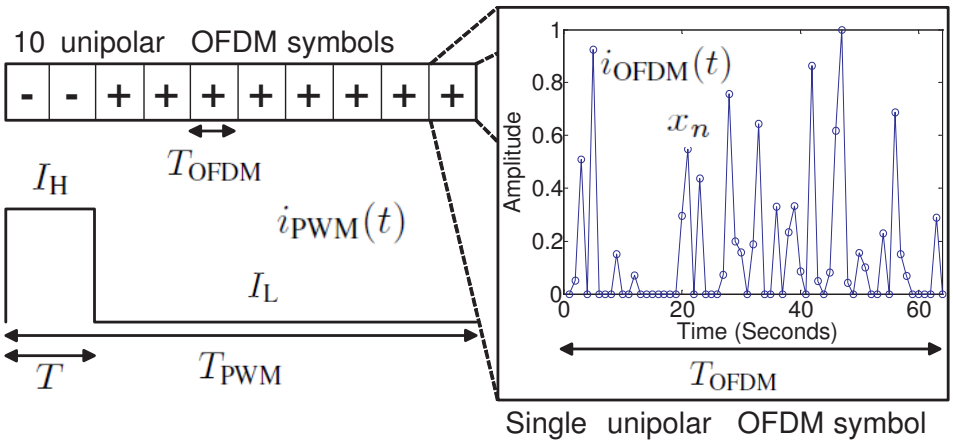

Figure 2: An example to demonstrate the proposed RPO-OFDM system: based on the dimming level, *i.e.* D, the polarity of the OFDM symbols are adjusted before the OFDM signal is superimposed on the PWM signal.

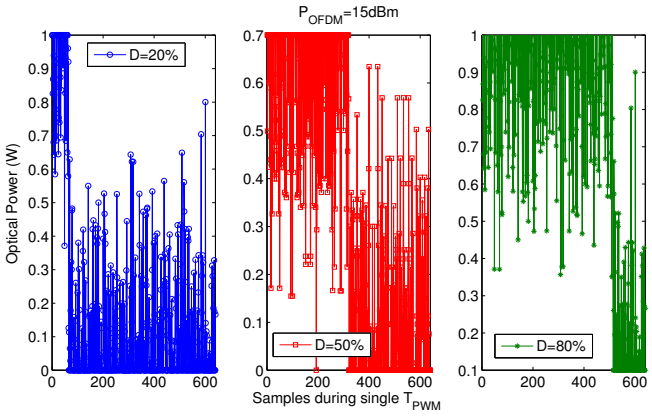

Figure 3: RPO-OFDM signals using 4-QAM and $P_{\text{OFDM}} = 15$dBm. Different D, I_{H} and I_{L}.

In reverse polarity optical OFDM (RPO-OFDM) system [16], $i_{\text{OFDM}}(t)$ is superimposed on $i_{\text{PWM}}(t)$ after setting a proper polarity of the individual OFDM symbols depending on whether the symbol is being transmitted on I_{H} or I_{L} during T_{PWM}. It is worth pointing out that RPO-OFDM can be applied to any unipolar OFDM version or the bipolar OFDM version, *i.e.* using two consecutive PWM periods per DCO-OFDM symbol. To explain the idea of RPO-OFDM with an example, $D = 20\%$, 10 ACO-OFDM symbols, $x_n = 64$ and $T_{\text{PWM}} = 10 \times T_{\text{OFDM}}$ are assumed. Consequently, the polarity of the first two ACO-OFDM symbols is reversed, *i.e.* -ve polarity, then transmitted on the I_{H} followed by 8 ACO-OFDM symbols, *i.e.* +ve polarity, transmitted on I_{L}. At the receiver side, and after time-synchronization, all 640 samples are extracted and the polarity of the first 128 samples is re-adjusted. Figure 3 shows different RPO-OFDM signals at an average OFDM signal power $P_{\text{OFDM}} = 15$dBm. Based on the target dimming level, *i.e.* D, the polarity is inverted.

The SNR for an undistorted OFDM signal is the ratio between the signal power and noise power and can be expressed as,

$$\text{SNR} \propto \frac{\sigma^2_{\text{OFDM}}}{\sigma^2_{\text{AWGN}}} \propto \frac{P_{\text{OFDM}}}{\sigma^2_{\text{AWGN}}} \tag{17}$$

where, σ^2_{AWGN} denotes variance of the additive white Gaussian noise (AWGN) representing shot and thermal noise at the reciever. Any DC optical power component or increase in D does not contribute to SNR improvement. The SNR can be improved only through maximizing σ^2_{OFDM}, *i.e.* determined by m.

If x_n is beyond DR_{LED}, $i_{\text{LED}}(t)$ will be clipped. By modeling this nonlinearity induced clipping noise as Gaussian noise, the effective SNR, SNR_{EFF} is given by:

$$\text{SNR}_{\text{EFF}} = \frac{\sigma^2_{\text{OFDM}}}{\sigma^2_{\text{AWGN}} + \sigma^2_{\text{C}}} \tag{18}$$

where, σ^2_{C} is the noise component due to clipping.

ϕ_{SB} can be controlled by adjusting D or jointly adjusting D and m. An optimum m is determined based on DR_{LED}, N and the target dimming range. Over one PWM period, I_{SB} is described as,

$$I_{\text{SB}} = D(I_H - \frac{mi}{N}\sum_{k=0}^{N-1} x_n) + (1-D)(I_L + \frac{mj}{N}\sum_{k=0}^{N-1} x_n) \tag{19}$$

where, i is the number of OFDM symbols transmitted during the "on-state" and j is the number of OFDM symbols transmitted during the "off-state". Assuming $I_L = 0$ and setting $D = 50\%$, it is clearly observed that I_{SB} is always equal to half the value of I_{H} and independent on m, *i.e.* σ^2_{OFDM}.

As for brightness, the human eye responds to lower ϕ_{SB} by enlarging the pupil, allowing more light to enter the eye. This response results in a nonlinear relation between measured and perceived light levels that is captured by the following formula:

$$\text{Perceived Light}(\%) = 100 \cdot \sqrt{\frac{\text{Measured Light}(\%)}{100}} \tag{20}$$

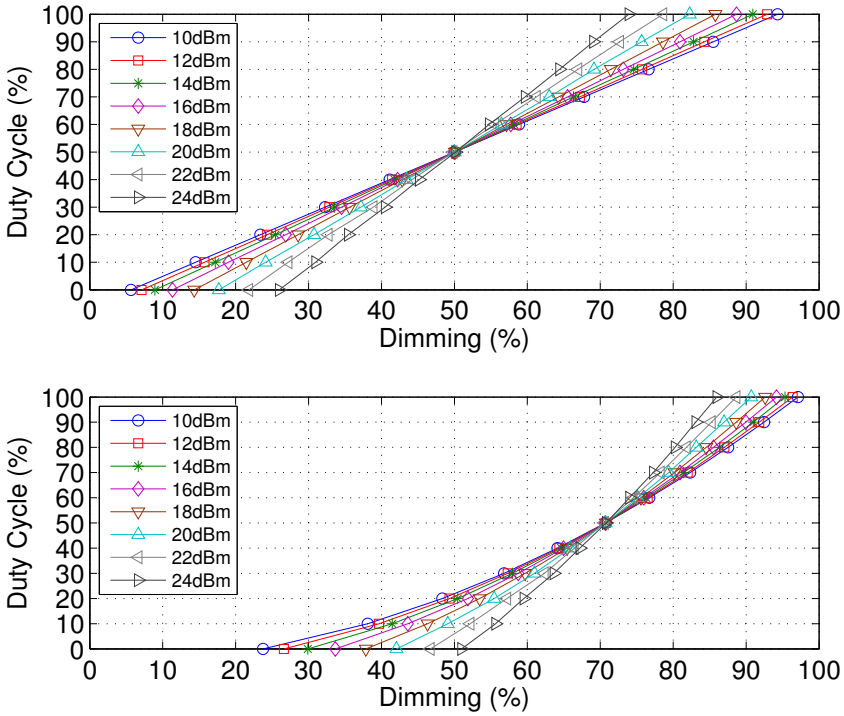

Figure 4: Optical dimming (upper) and perceived dimming (lower) as a function of D and P_{OFDM}.

5 Results

Simulations are conducted to investigate the influence of D and P_{OFDM} on the radiated optical power $\phi_{\text{LED}}(t)$, *i.e.* optical dimming, as well as the perceived LED brightness, *i.e.* perceived dimming. The dimming level is defined as a percentage of the maximum brightness, *i.e.* 100% dimming is full brightness. $I_{\text{H}} = 1A$, $I_{\text{L}} = 0A$ and P_{OFDM} are calculated over one ACO-OFDM symbol. Modulating signal current values above 1A are clipped. Figure 4 shows the obtained optical dimming and perceived dimming as a function of D. Curves are obtained at different values of P_{OFDM} that is incremented starting 10dBm up to 24dBm in steps of 2dBm. The numerical results confirm that the optical dimming can be linearly adjusted by varying D for different values of

P_{OFDM}. For large values of N (N>10), and due to the central limit theorem, the ACO-OFDM envelope can be accurately modeled as a Gaussian random process with zero mean. Thus at $D = 50\%$, P_{OFDM} has no effect on the dimming level. Further increase of P_{OFDM} narrows the dimming range around the 50% dimming. It is also highlighted that the human eye has better sensitivity at low luminance than high luminance. The nonlinear relation between optical dimming and perceived dimming is clearly observed. For instance, decreasing the optical power by 50% achieves only a 70% reduction in brightness.

The ICE at $D = 100\%$ is plotted in Fig. 5 as a function of DE and for different N. The upper x-axis shows the corresponding values of P_{OFDM}. The ICE is reduced with further increase of N, *i.e.* signal clipping probability increases as the PAPR gets higher. As shown in the subfigure (I_{SB} vs. P_{OFDM}), the I_{SB} approaches $\frac{I_{\text{H}}}{2}$ (0.5) as $\text{DR}_{\text{OFDM}} \gg \text{DR}_{\text{LED}}$. On the same subfigure, $P_{\text{OFDM}} = 25$dBm can be considered as an inflection point when clipping starts occurring and being dominant. At fixed DR_{LED}, the ICE decreases with increasing I_{SB}, *i.e.* reduction in P_{OFDM}. As DE approaches 1, ICE approaches $\frac{1}{\sqrt{\text{PAPR}}}$. Around DE $= 75\%$ ($P_{\text{OFDM}} = 25$dBm), ICE is about 25%. Beyond $P_{\text{OFDM}} = 25$dBm, signal clipping can be depicted by observing the degradation of the bit-error ratio (BER) performance in the subfigure (BER vs. P_{OFDM}). This BER is obtained assuming $\sigma^2_{\text{AWGN}} = 0$, *i.e.* only σ^2_{C} is considered.

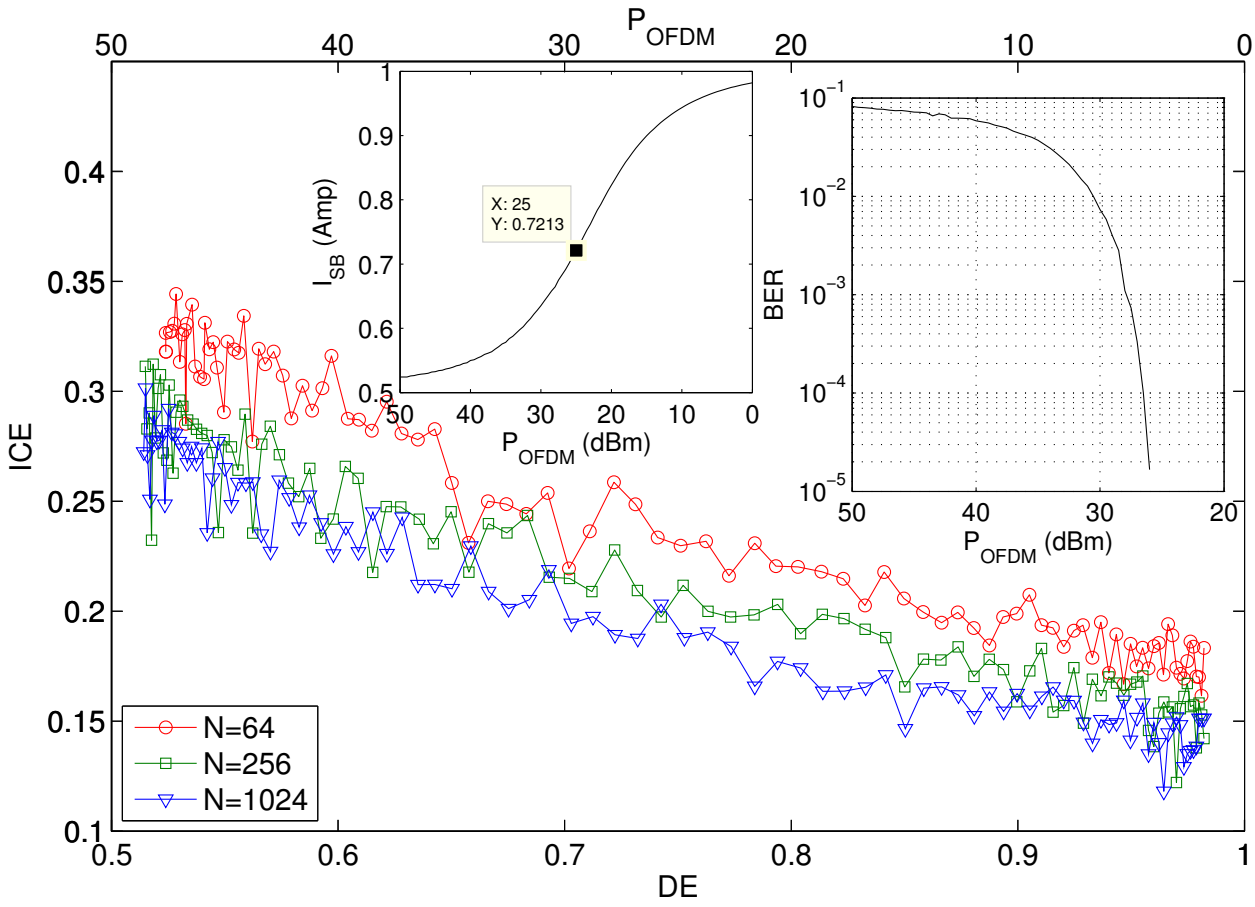

Figure 5: ICE vs. DE using 4-QAM and 2000 OFDM symbols per PWM period.

A proof-of-concept software defined VLC (SDVLC) testbed is realized as shown in Fig. 6. Matlab is used to build the RPO-OFDM system model, while Simulink is used to interface with the universal software radio peripheral (USRP) from Ettus Research. The transmitter frontend incorporates an illumination grade luminarie from Cree (the CR22 architectural LED troffer). We realized a real-time SDVLC implementation of the RPO-OFDM modulation techniques for dynamic adaptation to lighting conditions such that the $\phi_{\text{LED}}(t)$ is varied to meet illumination requirements. The Matlab-based GUI shows in almost real-time, for example, the number of bits in error per OFDM symbol and the estimated complex constellations.

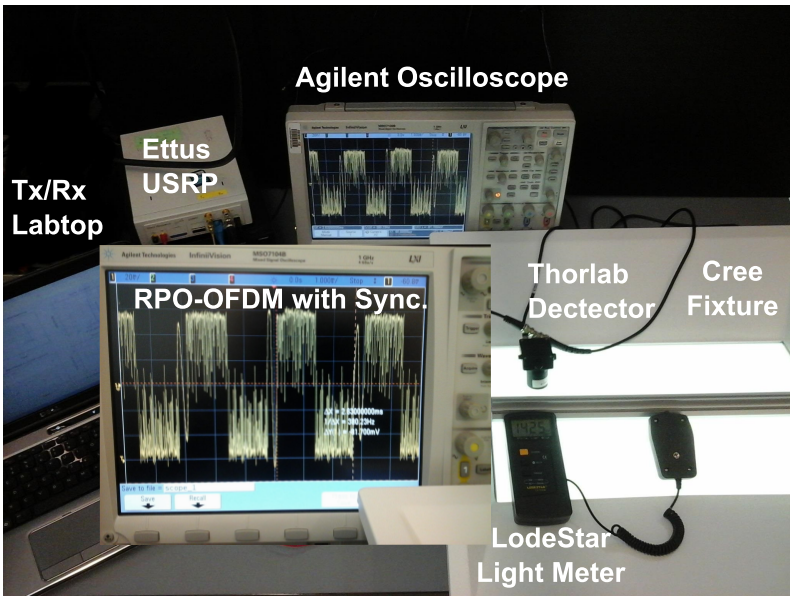

Figure 6: Proof-of-concept testbed showing $D = 50\%$ RPO-OFDM signal. A sinusoidal signal is used to realize a coarse Tx-Rx synchronization. Using 8 ACO-OFDM symbols per PWM period. For measurements, the optical detector and light meter are located directly on top of the LED troffer. The USRP2 equipped with the LFRX daughter board operating at 400KSps, a commercial photodetector (PDA36A from Thorlabs) equipped with a spherical concentrating lens and a LodeStar light meter are used.

Using the commercial optical detector and the digital light meter, the measured illuminance and BER are shown on Fig. 7 for different P_{OFDM}. It is experimentally confirmed that at a fixed P_{OFDM}, the obtained BER is maintained independent on the dimming level within the supported dimming range, *i.e.* the measured BER is 0, 4×10^{-4} and 2×10^{-3} at 17dBm, 13dBm and 10dBm, respectively. The reported BER is obtained without channel estimation and symbol equalization. The supported dimming range covers as low as 30%. It is also noticed that at around $D = 70\%$, P_{OFDM} has no effect on the dimming level, *i.e.* 2000lux which is at about 76% dimming relative to full brightness at about 2600lux. It is also experimentally confirmed that a higher P_{OFDM} narrows the dimming range.

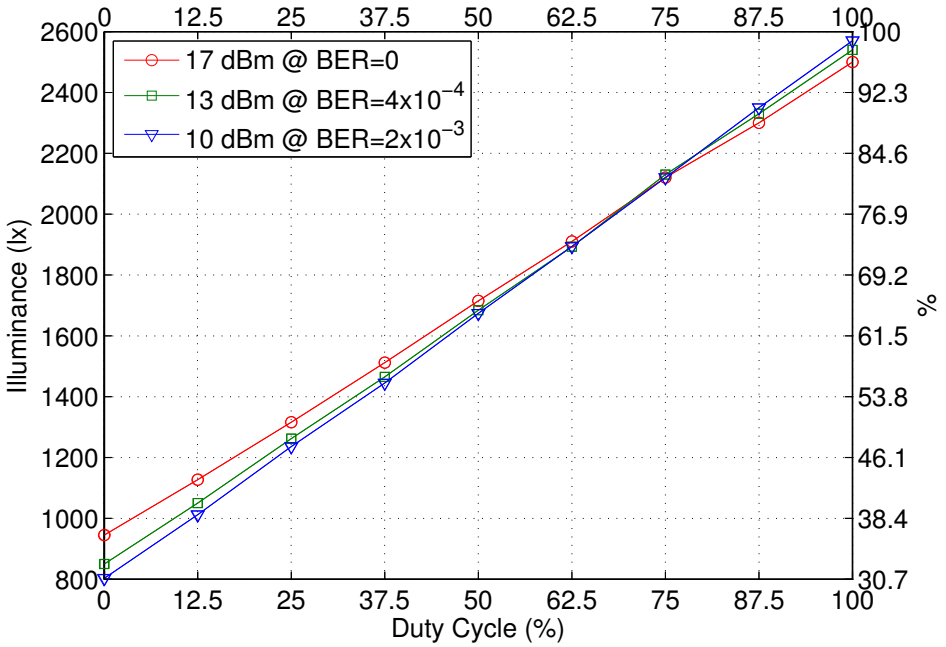

Figure 7: Illuminance vs. D at different P_{OFDM} and the corresponding BER.

6 Conclusion

By supporting the PWM dimming format, the new RPO-OFDM scheme based on a hybrid OFDM-PWM dimming has promise for speeding the adoption of the VLC technology into LED-based luminaries. Assuming an optimum OFDM signal power to maintain a target quality of service (QoS), the proposed approach decouples dimming for a wide-range from the performance, where both signals contribute to the effective LED brightness. Assuming that the PWM signal is utilizing the full LED dynamic range, the OFDM signal clipping is avoided for a wider amplitude-range of OFDM samples, *i.e.* the transmitted OFDM signal shape is preserved. In terms of spectral efficiency and bit-error performance, preserving the OFDM signal shape corresponds to less induced clipping noise allowing the use of high-order constellations (better spectral efficiency) or the establishment of more robust links (better BER).

References

[1] M. H. Crawford, "LEDs for solid-state lighting: performance challenges and recent advances," Selected Topics in Quantum Electronics, IEEE Journal of **15**(4), 1028–1040 (2009).

[2] C. DiLouie, *Advanced lighting controls: energy savings, productivity, technology and applications* (The Fairmont Press, Inc., 2006).

[3] E. F. Schubert, T. Gessmann, and J. K. Kim, *Light emitting diodes* (Wiley Online Library, 2005).

[4] H. Elgala, R. Mesleh, and H. Haas, "Indoor optical wireless communication: potential and state-of-the-art," Communications Magazine, IEEE **49**(9), 56–62 (2011).

[5] H. Elgala, R. Mesleh, and H. Haas, "Indoor broadcasting via white LEDs and OFDM," Consumer Electronics, IEEE Transactions on **55**(3), 1127–1134 (2009).

[6] H. Le Minh, Z. Ghassemlooy, D. O'Brien, and G. Faulkner, "Indoor gigabit optical wireless communications: challenges and possibilities," in ICTON, 1–6, (IEEE, 2010).

[7] J. Vucic and K.-D. Langer, "High-speed visible light communications: State-of-the-art," in OFC/NFOEC, 1–3, (IEEE, 2012).

[8] R. Mesleh, H. Elgala, and H. Haas, "Performance analysis of indoor OFDM optical wireless communication systems," in WCNC, 1005–1010, (IEEE, 2012).

[9] E. Pisek, S. Rajagopal, and S. Abu-Surra, "Gigabit rate mobile connectivity through visible light communication," in ICC, 3122–3127,(IEEE, 2012).

[10] Z. Wang, W.-D. Zhong, C. Yu, J. Chen, C. P. S. Francois, and W. Chen, "Performance of dimming control scheme in visible light communication system," Optics Express **20**(17), 18861–18868 (2012).

[11] G. Ntogari, T. Kamalakis, J. Walewski, and T. Sphicopoulos, "Combining illumination dimming based on pulse-width modulation with visible-light communications based on discrete multitone," Journal of Optical Communications and Networking **3**(1), 56–65 (2011).

[12] J. Armstrong and B. J. Schmidt, "Comparison of asymmetrically clipped optical OFDM and DC-biased optical OFDM in AWGN," Communications Letters, IEEE **12**(5), 343–345 (2008).

[13] J. Gancarz, H. Elgala, and T. D. C. Little, "Impact of lighting requirements on VLC systems," Communications Magazine, IEEE **51**(12), 34–41 (2013).

[14] Y. Gu, N. Narendran, T. Dong, and H. Wu, "Spectral and luminous efficacy change of high-power LEDs under different dimming methods," Proc. SPIE **6337**, 63370J–63370J-7 (2006).

[15] H. Elgala , R. Mesleh and H. Haas, "Modeling for predistortion of LEDs in optical wireless transmission using OFDM," in HIS, 12–14,(IEEE, 2009).

[16] H. Elgala and T. D. C. Little, "Reverse Polarity Optical-OFDM (RPO-OFDM): Dimming Compatible OFDM for Gigabit VLC Links," Optics Express **21**(20), 24288–24299 (2013).